Stereoscopic imaging through scattering media

David Abookasis and Joseph Rosen

Department of Electrical and Computer Engineering, Ben-Gurion University of the Negev, P.O. Box 653, Beer-Sheva 84105, Israel

Received July 5, 2005; revised November 18, 2005; accepted November 30, 2005; posted December 5, 2005 (Doc. ID 63244)

We develop and experimentally test a method for three-dimensional imaging of hidden objects in a scattering medium. In our scheme, objects hidden between two biological tissues at different depths from the viewing system are recovered, and their three-dimensional locations are computed. Analogous to a fly's two eyes, two microlens arrays are used to observe the hidden objects from different perspectives. At the output of each lens array we construct the objects from several sets of many speckled images with a previously suggested technique that uses a reference point. The differences of the reconstructed images in both arrays with respect to the reference point yield the information regarding the relative depth among the various objects.

OCIS codes: 110.6880, 030.6140.

Medical tomography techniqes such as x-ray computed tomography[1] (CT) offer great advantages and are still widely used despite the fact that they suffer from several drawbacks such as ionizing radiation, a complex structure, and high cost. The advantage of optical tomography over other medical tomography techniques is that they provide quantitative information on functional properties of tissues while being nonharmful (the radiation is nonionizing). Accordingly, in recent years researchers have invested considerable effort toward developing optical tomography systems that use near-infrared light. In the present study we suggest a simple optical tomography technique that is based on speckled images. The proposed system is an extension toward three-dimensional (3D) imaging of our previous works, referred to as noninvasive optical imaging by speckle ensemble[2,3] (NOISE) and its modified version[4] NOISE-2. Therefore we term the present technique NOISE-3D.

In this Letter we extend NOISE-2 to develop a new imaging technique for embedding objects in a scattering medium. In addition to reconstructing the object, its location in the 3D space is also extracted. Therefore the proposed system has the advantage of revealing and acquiring depth information of objects seen through a scattering medium.

Figure 1 is a schematic diagram of the proposed 3D imaging system. The configuration consists of two microlens arrays (MLAs) accompanied by imaging lenses, a pinhole (implemented by an adjustable iris) placed behind the second scattering layer T_2. Each path, left and right separately, is equivalent to that given in Ref. 4. However, it should be noted that, unlike NOISE-2, in the present setup the point source is placed in front of the scattering medium, and thus serves as a reference point instead of as a point source of illumination. We find that this change improves the reconstructed image because now light from the pinhole is no longer scattered. Therefore the pinhole's image is narrower and so is its cross correlation with the object's image. The idea behind this point technique is to ascribe the location of an object to a location of some known point in space. The computational process at each channel is schematically described in the lower part of Fig. 1. As in NOISE-2, the computational process yields three spatially separated terms at the output of each path. One term is the zero order at the vicinity of the output plane origin. This term is equal to the sum of the pinhole autocorrelation and the object autocorrelation. The other two terms correspond to the cross correlation between the object and the pinhole and thus, assuming the average pinhole image is close to a point, these terms approximately yield the object recon-

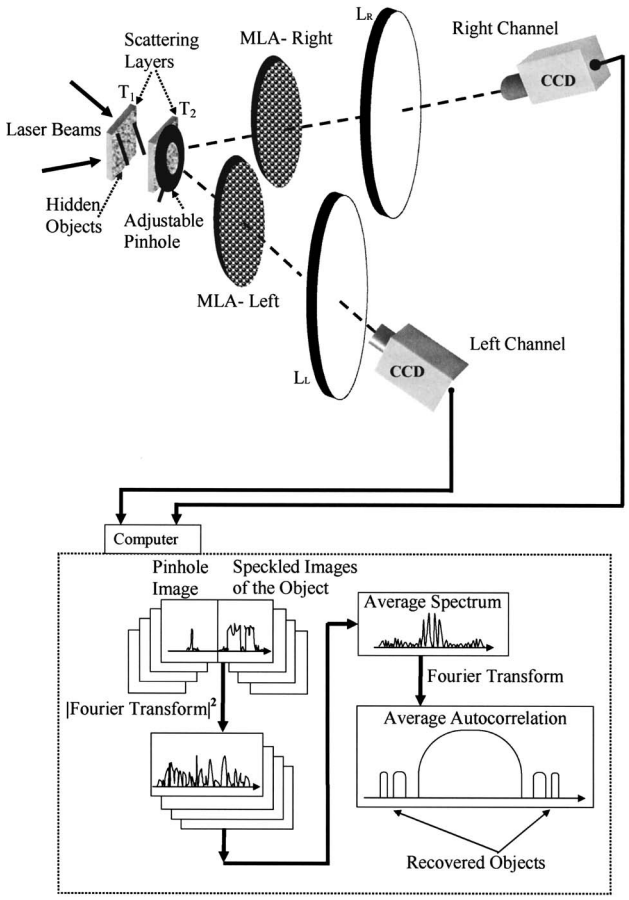

Fig. 1. Schematic diagram of the proposed stereoscopic NOISE system. The lower block diagram describes the computational process of each channel.

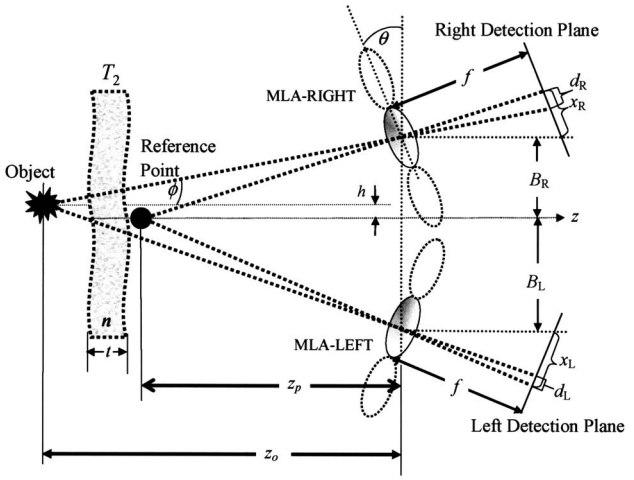

Fig. 2. Perspective projection geometry of the object and the reference point through each channel.

struction. The image of the hidden object can therefore be retrieved by reading it from one of these orders. Note that in this scheme the distance of the reconstructed object from the output plane origin is related directly to the transverse gap between the object and the reference point.

To extract the depth information about the object we initially use the principle of stereoscopic vision, ignoring, for the time being, the effect of the scattering medium T_2. In the diagram depicted in Fig. 2, the projection of the object and the point reference on the image planes of both arrays can be presented as follows:

$$\frac{x_{R,L}\cos\theta}{f} \cong \frac{B_{R,L}}{z_p}, \quad \frac{(x_{R,L}-d_{R,L})\cos\theta}{f} \cong \frac{B_{R,L}\mp h}{z_o}, \tag{1}$$

where z_o and z_p are the distance of the object and the pinhole from the center of the array, respectively. B_R and B_L represent the distance of each array from the z axis. d_R and d_L are the gaps between the images of the reference point and the observed object, in the right and left channels, respectively. x_R and x_L are the displacements of the reference point images from the horizontal axis that crosses the center of each microlens, in the right and left channels, respectively. h is the transverse gap between the object and the pinhole, and θ is the tilt angle of each array. Solving the four equations of Eqs. (1) yields the distance between each array plane to the object, given by

$$z_o = \frac{Bfz_p}{Bf - z_p D\cos\theta}, \tag{2}$$

where $B=B_R+B_L$ is the baseline and $D=d_R+d_L$ is the sum of the object-reference point gaps at the two channels. It is clear from Eq. (2) that different perspectives lead to a slight displacement of the object in the two views of the scene. Equation (2) has the advantage that one needs only to measure D that is related to the sum of the distances of the reconstructed object from the output plane origin at the two channels. Accordingly, we achieve a simple method for obtaining the object's depth since in our configuration the baseline B, the focal length f, and the pinhole distance from the MLA z_p are known parameters. Calculating D, as described below, we can estimate the depth information, z_o, of an object from the MLAs in an imaged scene. Note that by using the pinhole there is no need to know the object and the reference point locations that are difficult to estimate in such a noisy scattering system. This is an additional advantage of using a method with a reference point.

Since objects are covered under layer T_2 with a higher-than-one index of refraction, while the reference point is positioned in front of T_2, the obtained gap between each object and the reference point in each channel is different from the situation without the layer T_2. Considering Snell's law and the fact that layer T_2 is tilted relative to the optical axis of each array, the corrected displacement D from the measured displacement $\tilde{D}$ is

$$D = \tilde{D} + \frac{2ft\sin\phi}{z_o}\left(1 - \frac{\cos\phi}{\sqrt{n^2-\sin^2\phi}}\right), \tag{3}$$

where $\tilde{D}=\tilde{d}_R+\tilde{d}_L$ is the sum of the object-reference point gaps at the two channels measured after introducing layer T_2; t and n are the thickness and the refractive index of the scattering layer, respectively; and ϕ is the angle between the z axis and the ray connecting the centers of the object and the MLA. The second term in Eq. (3) describes the size change of the image as a consequence of layer T_2. Since ϕ and z_o are unknown before calculating Eqs. (1), ϕ and z_o are initially approximated as θ and z_p, respectively, to yield an initial estimation for D. In case other parameters of the setup such as the orientation, thickness, and index of refraction of the scattering layers are unknown, more sophisticated methods for estimating these parameters should be applied. However, these methods are out of the scope of this Letter.

The next step is to extract the information about the displacement $\tilde{D}$ from the reconstructed image. According to the technique of NOISE-2 (depicted in the flow chart of Fig. 1) for each path, each subimage of the speckled point reference with a corresponding subimage of the object (recorded by a different exposure where the iris is opened) is Fourier transformed and the square magnitude of each subspectrum is accumulated with all the other subspectrums. This average joint power spectrum is then Fourier transformed, which yields the output correlation plane. This plane in turn yields a symmetric image reconstruction around the plane origin. By taking one of the first orders, we count the number of pixels that range from this order to the plane origin. The distance in pixels is converted to a real distance at the arrays' image plane by subtracting the submatrix width, by multiplying the pixel number with the size of the CCD pixel, and by dividing the result by the magnification of the imaging lenses L_R and L_L. These operations are performed on each path to estimate $\tilde{D}$.

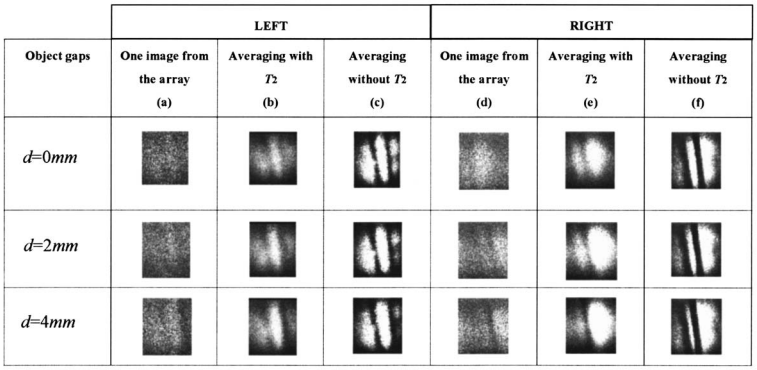

Fig. 3. Summary of the imaging results obtained by NOISE-3D.

By calculating D using Eq. (3) we can now calculate the object depth by using Eq. (2).

Experiments with two separated cylindrical sticks as observed objects were carried out by using the configuration shown in Fig. 1. The sticks had a length of 20 mm and a diameter of 2.1 mm each. During the experiments, the left stick was constantly attached to tissue T_1 while the right stick was moved longitudinally toward the MLAs, at three different positions. Thus the relative longitudinal displacements between the sticks were 0 mm (the objects are at the same plane), 2 mm, and 4 mm. The sticks were embedded between two slabs of chicken breast separated by a distance of 12 mm. This scattering medium is characterized by a scattering coefficient of $\mu_s = 128 \pm 9\ \mathrm{cm}^{-1}$ (see Ref. 3) and absorption coefficient of $\mu_a \approx 0.2\ \mathrm{cm}^{-1}$.[5] The thicknesses of the rear tissue T_1 and the front tissue T_2, were approximately 3 and 4.5 mm, respectively. The reference point was created by placing a pinhole with an adjustable aperture at a short distance (22 mm) behind tissue T_2, between T_2 and the MLAs. The rear tissue T_1 was illuminated by two diagonal collimated plane waves emerging from the He–Ne laser at 632.8 nm with 35 mW. The two MLAs were placed at a distance of $z_p = 162$ mm from the pinhole. Each MLA consists of 42×42 microlenses, but only 3×8 were used in this experiment. Using more than three columns per channel introduces a considerably different perspective of the object into the averaged image, and thus the reconstructed image is degraded. The diameter of each microlens is 0.6 mm, and its focal length is 6.3 mm. The image plane of each MLA is projected onto the CCD plane by a single spherical lens L_L or L_R, respectively, each with a focal length of 120 mm and a diameter of 150 mm. These lenses, with a magnification of 1.3, match the MLA size with the CCD size. At each channel the distance from the MLA to the imaging lens is 210 mm, and the distance from the MLA to the CCD plane is 280 mm. The baseline B is 80 mm. After we acquired the sets of the observed image in each path, a computer program was employed to reconstruct the sticks and to determine their distance from the MLAs according to Eqs. (2) and (3).

A summary of all the results is displayed in Fig. 3. Columns (a) and (d) show typical subimages obtained from a typical microlens without using the averaging process. The reconstructed images derived from the averaging process on the images of the hidden sticks with different relative displacements between the objects are shown in column (b) for the left channel and column (e) for the right channel. Note that the reconstruction of one of the sticks (the right one from Fig. 1) in the pictures is improved as a consequence of its closeness to scattering layer T_2, while the other stick (the left one from Fig. 1) remains far from T_2. Columns (c) and (f) show the same reconstructed images obtained by removing the second tissue, T_2, from the same setup. The effect of stereoscopic vision is clearly demonstrated in these figures by observing that in the right path the relative distance between the sticks gets smaller while in the left path the distance grows as a consequence of moving the right stick longitudinally toward the MLAs.

Measuring corresponding distances in different figures can succeed only when there are well-seen indicators on the objects that are viewed from the two channels. In our almost vertical sticks we choose to refer to the central point of each stick as the object point for the distance measurements. By using these measurements, and applying Eqs. (2) and (3), our results indicate that the relative distances between the sticks without taking T_2 into account, measured in Figs. 3(c) and 3(f), are 0.302, 2.414, and 4.397 mm instead of real distances of 0, 2, and 4 mm. Taking T_2 into account, the relative distances between the sticks, measured in Figs. 3(b) and 3(e), are 0.24, 2.358, and 4.548 mm. The average error in measuring z_o is less than 0.1%.

This research was supported by Israel Science Foundation grant 119/03. J. Rosen's e-mail address is rosen@ee.bgu.ac.il.

References

1. J. G. Webster, *Minimally Invasive Medical Technology* (Institute of Physics, 2001), Chap. 4, pp. 46–58.
2. J. Rosen and D. Abookasis, Opt. Express **11**, 3605 (2003).
3. J. Rosen and D. Abookasis, Opt. Lett. **29**, 253 (2004).
4. D. Abookasis and J. Rosen, Opt. Lett. **29**, 956 (2004).
5. G. Marquez, L. V. Wang, S.-P. Lin, J. A. Schwartz, and S. L. Thomsen, Appl. Opt. **37**, 798 (1998).